PHYSICAL REVIEW A, **66**, 021801(R) (2002)

Extreme-ultraviolet high-order harmonic pulses in the microjoule range

J.-F. Hergott, M. Kovacev, H. Merdji, C. Hubert, Y. Mairesse, E. Jean, P. Breger, P. Agostini, B. Carré, and P. Salières
CEA/DSM/DRECAM, Service des Photons, Atomes, et Molécules, Centre d'Etudes de Saclay, 91191 Gif-sur-Yvette, France
(Received 16 April 2002; published 20 August 2002)

We study high-order harmonic generation at a high pumping energy using a long focal length lens. We identify different saturation regimes of the harmonic emission, revealing the interplay between phase matching, absorption, and laser defocusing. In the optimal conditions, high conversion efficiencies are obtained, resulting in an increase of at least one order of magnitude of the harmonic energies compared to previously reported values. In xenon, microjoule energies are reached, opening new perspectives for the applications of this ultrashort coherent radiation.

DOI: 10.1103/PhysRevA.66.021801 PACS number(s): 42.65.Ky, 32.80.Rm

The generation of the high-order harmonics of intense laser pulses in gases [1] has recently opened new perspectives for probing matter in the extreme-ultraviolet (XUV) pulses on an unprecedented time scale. The ultrashort harmonic pulse duration is used in pump-probe experiments in atomic [2,3] and molecular [4–6] spectroscopy, as well as in solid-state physics [7,8]. Combined to the high intrinsic beam coherence, it has allowed ultrafast diagnosis of laser-produced plasmas through XUV interferometry [9,10]. However, the harmonic beam energy is still relatively low and many applications would become possible if the number of generated photons were increased: ultrafast XUV holography, diagnosis of dense bright plasmas, or even study of nonlinear processes in the XUV, limited so far to low harmonic orders [11]. Recently a number of studies have demonstrated high conversion efficiencies, using ultrashort laser pulses focused in hollow core fibers [12–14] or cells [15,16]. However, these efficiencies were obtained at a very low laser energy (less than 1 mJ in most cases) that imposed a relatively tight focusing geometry in order to reach saturation intensities of the generating rare gases. This resulted in a low harmonic energy, in the nanojoule range. The fact that much larger energies are now available on ultrashort laser systems raises a number of questions: using higher laser energies and looser focusing, is it possible to achieve similar efficiencies, and thus to generate microjoule harmonic pulses? In particular, how will phase matching be affected by these unusual generating conditions?

In this Rapid Communication, we report a thorough study of harmonic generation at a high pumping energy using a long focal length lens. Using a pumping energy of 27 mJ and a $f=2$ m lens, we study the influence of the beam aperture, the medium length, and the atomic density on the harmonic yield produced in a pulsed gas jet. We identify different saturation regimes, thanks to the excellent quantitative agreement obtained with detailed three-dimensional (3D) simulations. In particular, we clearly observe the interplay between phase matching, absorption, and defocusing, the main limiting factors of the macroscopic emission. Absolute photon number measurements in the optimal conditions give conversion efficiencies as high as those reported using ultrashort (<20 fs) laser pulses, but now with ten times more energy. Using a $f=5$ m lens, we show that even higher conversion efficiencies can be obtained, resulting in harmonic energies in excess of 1 μJ.

The experiments were performed on the LUCA laser facility with an amplified Ti:sapphire system delivering 60 fs pulses at 800 nm, with an energy of up to 100 mJ at 20 Hz. In our experiment, a pumping energy of 27 mJ was focused with either a $f=2$ m or 5 m lens in a pulsed gas jet. The nozzle was formed by a slit of dimensions 300 μm$\times$3 mm producing a jet at pressure 10–100 Torr characterized by Mach-Zehnder interferometry. By rotating the jet relative to the laser axis, we can change the length of the generating medium, while keeping the same peak density. Harmonics produced in the jet are analyzed by an XUV spectrometer without entrance slit [17], and detected with a calibrated XUV photodiode blinded for diffused IR light with two 100 nm Al filters. The absolute spectrometer response (as well as the filter transmission) was measured using the harmonic radiation as a source further monochromatized with another spectrometer, like a synchrotron beam line.

Since the total aperture of the laser beam was 40 mm, the intensity at the focus of the 2 m lens reached 4×10^{15} W/cm^2 (the laser beam is two times diffraction limited). This is much above the saturation intensity of rare gases, and results in a low harmonic signal due to ionization effects: depletion of the generating medium, strong free-electron dispersion implying poor phase matching. The first step to optimize the harmonic yield was to control the laser aperture and the jet/focus position [18–20]. Closing a diaphragm placed before the lens means both decreasing the laser energy and increasing the focal spot size, therefore fastly decreasing the focal intensity. In all gases, we observe a strong increase of the harmonic signal (even stronger increase of the conversion efficiency) followed by a decrease for a too small aperture size. In xenon, the optimal size was 13 mm corresponding to 4.3 mJ laser energy and an intensity of 8×10^{13} W/cm^2, in argon, 15 mm (5 mJ and 1.4×10^{14} W/cm^2), in neon, 19 mm (8.5 mJ and 3.7×10^{14} W/cm^2). These apertures optimize the spatial repartition of the laser energy in each gas: a high enough intensity (slightly below the saturation intensity) over a large emitting volume (focal spot diameter between 350 and 530 μm). In general, the optimal jet position was a few cm (2.5) before the focus.

In a second step, we studied the combined influence of the pressure [21] and medium length [22] at the optimal laser aperture. In Fig. 1 is shown the pressure dependence of dif-

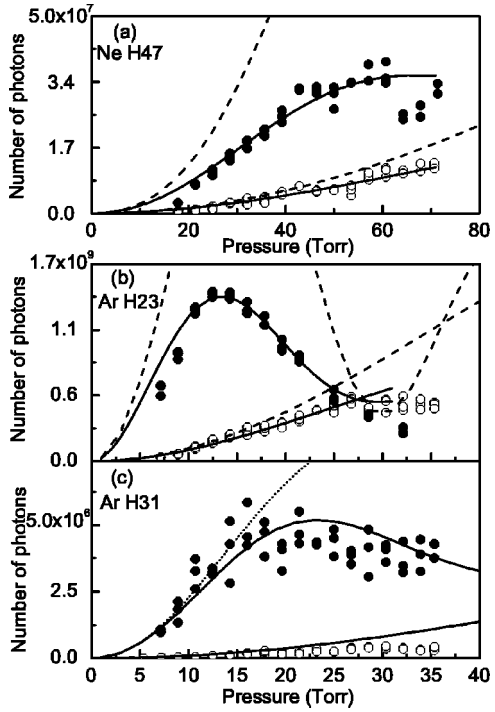

FIG. 1. Pressure dependence of H47 in neon (a), H23 (b), and H31 (c) in argon for a medium length of 0.5 mm (open circles) or 2.5 mm (solid circles). Curves are simulation results: full (solid) lines, without absorption [dashed lines in (a) and (b)]; without laser defocusing [dotted line in (c)].

ferent harmonics for two medium lengths: 0.5 mm (open circles) and 2.5 mm (solid circles). In all cases, the harmonic signal in the short medium is weak and increases slowly with pressure. In contrast, in the long medium, it increases steeply and saturates at high pressure [47th harmonic (H47) in neon and H31 in argon] or shows a marked decrease after an optimum at 13 Torr in the case of H23 in argon. These variations of the harmonic yield can be interpreted using a 1D model [13], through the relative value of the different characteristic lengths. The harmonic field builds up constructively over the coherence length defined by $L_{coh}=\pi/|\Delta\vec{k}|$, where $\Delta\vec{k}=\vec{k}_q-q\vec{k}_1$ is the wave vector difference of the harmonic and polarization fields. This phase matching factor is determined by the different dispersion terms. The atomic dispersion has a sign opposite to the electronic and geometric (Gouy phase) dispersions and can thus compensate them at a particular pressure. In the strong field regime, the ''intrinsic'' phase of the harmonic dipole introduces an additional dispersion term proportional to the gradient of the laser intensity I [23]. The pressure dependence of the resulting coherence length is illustrated by solid line in Fig. 2 in the case of H47 generated in neon. For a pressure of 60 Torr, the dispersion terms cancel out, leading to an infinite coherence length.

The second characteristic length is the absorption length (shown by dot-dashed line in Fig. 2), defined by $L_{abs}=1/\sigma\rho$, where σ is the photoionization cross section and ρ the gas density. Finally the reference length is the medium length L_{med}. Constant *et al.* [13] worked out a rule of thumb for optimizing harmonic emission in the form of two conditions: $L_{med}>3L_{abs}$ and $L_{coh}>5L_{abs}$. In the short medium, the first condition is not fulfilled and the emission is limited by the medium length. In contrast, in the long medium, there is a pressure range from 55 to 115 Torr where both conditions can be fulfilled simultaneously. This leads to an absorption limited emission explaining the saturation of the harmonic signal in Fig. 1(a). A similar analysis can be performed for H23 and H31 generated in argon. However, this 1D model does not account for the radial phenomena occuring during the propagation of the fields that may affect significantly the harmonic yield, such as defocusing of the laser beam by a strong electron density gradient, or off-axis phase matching of the harmonic beam. Indeed, both ionization and intrinsic dipole phase strongly depend on intensity and thus on space in the focal volume and on time in the laser envelope.

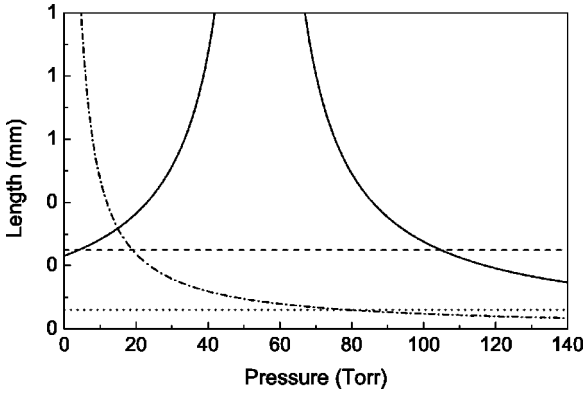

FIG. 2. Calculated absorption length (dot-dashed line) and coherence length (solid line) for H47 generated in neon at 4×10^{14} W/cm^2 [laser beam ($b=9$ cm) focused 2.5 cm after the jet, ionization rate 0.3%, dipole phase αI with $\alpha=20\times10^{-14}$ rad W^{-1} cm^2]. Medium lengths of 0.5 mm (2.5 mm) are indicated in dotted (dashed) lines.

Detailed 3D simulations are thus necessary to interpret unambiguously the saturation of the harmonic yields in Fig. 1. We used the harmonic dipoles calculated from the strong field approximation approach of Lewenstein *et al.* [24], the Ammosov-Delone-Krainov tunneling ionization rates [25], and a 3D propagation code [26] accounting for all the ionization effects (defocusing, depletion, phase mismatch), as detailed in Ref. [1]. The results are shown in solid lines in Fig. 1. An excellent agreement with the experimental curves is obtained in neon and argon. Note that while the absolute scale of the simulated data has been adjusted to match the experimental ones, the ratio between the short and long medium results has not been modified, providing us with a stringent test of the simulations. If we switch off the absorption in the code, we get the curves shown by dashed lines in Figs. 1(a) and 1(b). In the short medium, the influence of absorption is quite small, indicating that the medium length is the limiting factor. In contrast, for the long medium, there is a large deviation of the curves at the optimal pressures, indicating that an absorption limited emission is reached. In the case of H23 in argon, phase mismatch takes over at high pressure, resulting in a strong decrease in the harmonic signal due to destructive interference in the medium. To our

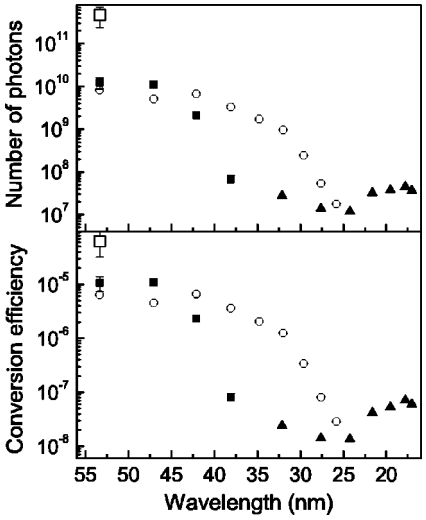

FIG. 3. Absolute number of harmonic photons per pulse (a) and corresponding conversion efficiencies (b) obtained in xenon (solid squares), argon (open circles), and neon (solid triangles) with the 2 m lens. The open squares show the result with the 5 m lens.

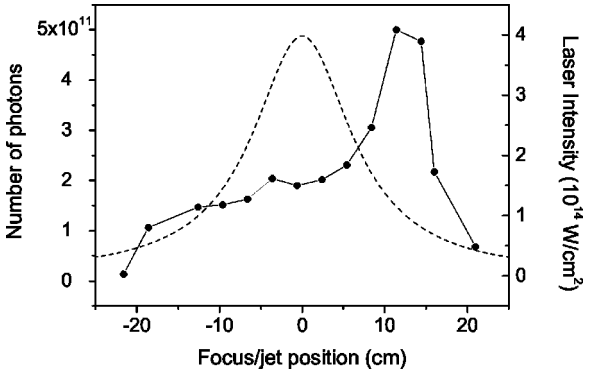

FIG. 4. Number of photons of H15 generated in xenon (80 Torr) with 25 mJ laser energy as a function of the position of the focus relative to the jet. The dotted line indicates the laser intensity in vacuum (right scale).

knowledge, this is the first time that the interplay between absorption and phase matching is so clearly observed and simulated. Note finally that the optimal phase matching pressures in neon (60 Torr) and argon (13 Torr) are smaller than most of those reported using tighter focusing [12,15,27]. This indicates that the geometric dispersion, though diminished by the looser focusing, still plays an important role in phase matching.

Despite the similar shapes of the curves, the case of H31 generated in argon is very different from the former ones. Removing the absorption barely modifies the pressure dependence in the long medium. Indeed, the absorption cross section at this wavelength (close to the Cooper minimum) is very small, resulting in an absorption length of 1 cm at 25 Torr. According to the 1D model, the saturation of the yield obtained in the long medium would be thus attributed to a finite coherence length. In fact, this is the result of the laser defocusing and subsequent decrease of intensity [21] since when this is not taken into account [dotted lines in Fig. 1(c)], the yield increases steeply in the long medium and does not show any saturation in this pressure range. The limiting factor becomes thus the amplification length L_{amp} over which the dipole amplitude remains high. Since H31 in the cutoff of the spectrum is very sensitive to intensity variations, the fluctuations of I amplified by the defocusing lead to scattered experimental points at high pressure.

The number of harmonic photons generated in the optimized conditions, and the corresponding conversion efficiencies are displayed in Fig. 3. The efficiency reaches 10^{-5} for harmonics in the plateau of xenon, 7×10^{-6} in argon and close to 10^{-7} in neon. These values compare well with those obtained with ultrashort (<20 fs) laser pulses [12,15], because the intermediate orders considered are generated efficiently below the saturation intensity (high orders in the cutoff region of course need short laser pulses to reach the plateau and thus a high conversion efficiency). Since we use a few mJ instead of a few 100 μJ of laser energy, we generate at least ten times more photons. The largest photon number (10^{10}) is obtained for H15 generated in xenon. In this case, the pressure dependences in the short and long medium were similar with a saturation around 80 Torr, indicating an absorption-limited emission already in the short medium.

In order to push these results further, we changed for a $f=5$ m lens to increase even more the focal spot size, using as much laser energy as available. The xenon jet was positioned perpendicularly to the laser axis, providing a large transverse density profile. The optimal laser aperture (33 mm) resulted in a similar f number as for $f=2$ m but a much larger energy (25 mJ), i.e., a focal intensity above saturation. The optimal jet position is then obtained for a focusing 11 cm after the medium, as shown in Fig. 4. At this position, the laser spot diameter is about 1 mm, corresponding to an intensity of 1.2×10^{14} W/cm^2 slightly above saturation in xenon. $5\pm2.5\times10^{11}$ photons are generated (open square in Fig. 3), corresponding to an harmonic beam energy of 1.9 ± 0.9 μJ per pulse. This is more than one order of magnitude larger than all previously reported values. Moreover, while the harmonic energy is increased by 40, the pump energy is only increased by 6 (and the intensity by 1.7). The conversion efficiency is therefore enlarged by a factor 6 ± 3. The simple scaling of the pump energy and the focal spot size [28] cannot account for such a growth whose cause must be sought in the higher intensity where an absorption-limited phase-matched emission is realized [29]. This is made possible thanks to the laser defocusing by the free-electron density gradient: when the laser is focused before the medium, its natural divergence is increased, resulting in a small L_{amp}. When focused after the jet, the laser convergence is reduced, resulting in a uniform intensity and phase distribution due to channeling [30].

In conclusion, we have shown that high conversion efficiencies can be obtained at high laser pumping energies using long focal length lenses, resulting in an increase of at least one order of magnitude of the harmonic energies compared to the previously reported values. This is obtained by controlling the laser aperture, length, pressure, and position

of the gas medium. In xenon, microjoule energies are obtained for the 15th harmonic beam. This opens new perspectives for the applications of harmonic radiation, all the more so as it is obtained with standard equipment (60 fs 30 mJ laser, pulsed jet) available in many laboratories.

We thank P. Troussel and G. de Lachèze-Murel for lending us the calibrated photodiode. M. K. acknowledges the financial support provided through the European Community's Human Potential Programme under Contract No. HPRN-CT-2000-00133, ATTO.

[1] P. Salières *et al.*, Adv. At., Mol., Opt. Phys. **41**, 83 (1999).
[2] J. Larsson *et al.*, J. Phys. B **28**, L53 (1995).
[3] M. Gisselbrecht *et al.*, Phys. Rev. Lett. **82**, 4607 (1999).
[4] S.L. Sorensen *et al.*, J. Chem. Phys. **112**, 8038 (2000).
[5] M. Bauer *et al.*, Phys. Rev. Lett. **87**, 025501 (2001).
[6] L. Nugent-Glandorf *et al.*, Phys. Rev. Lett. **87**, 193002 (2001).
[7] R. Haight *et al.*, Phys. Rev. Lett. **70**, 3979 (1993).
[8] F. Quéré *et al.*, Phys. Rev. B **61**, 9883 (2000).
[9] P. Salières *et al.*, Phys. Rev. Lett. **83**, 5483 (1999).
[10] D. Descamps *et al.*, Opt. Lett. **25**, 135 (2000).
[11] Y. Kobayashi *et al.*, Opt. Lett. **23**, 64 (1998).
[12] A. Rundquist *et al.*, Science **280**, 1412 (1998).
[13] E. Constant *et al.*, Phys. Rev. Lett. **82**, 1668 (1999).
[14] R. Bartels *et al.*, Nature (London) **406**, 164 (2000).
[15] M. Schnürer *et al.*, Phys. Rev. Lett. **83**, 722 (1999).
[16] Y. Tamaki *et al.*, Phys. Rev. Lett. **82**, 1422 (1999).
[17] A. L'Huillier *et al.*, Phys. Rev. Lett. **70**, 774 (1993).
[18] Ph. Balcou *et al.*, J. Phys. B **25**, 4467 (1992).
[19] J.J. Macklin *et al.*, Phys. Rev. Lett. **70**, 766 (1993).
[20] T. Ditmire *et al.*, Phys. Rev. A **51**, R902 (1995).
[21] C. Altucci *et al.*, J. Opt. Soc. Am. B **13**, 148 (1995).
[22] C. Delfin *et al.*, J. Phys. B **32**, 5397 (1999).
[23] P. Salières *et al.*, Science **292**, 902 (2001).
[24] M. Lewenstein *et al.*, Phys. Rev. A **49**, 2117 (1994).
[25] M.V. Ammosov *et al.*, Zh. Eksp. Teor. Fiz. **91**, 2008 (1986) [Sov. Phys. JETP **64**, 1191 (1986)].
[26] A. L'Huillier *et al.*, Phys. Rev. A **46**, 2778 (1992).
[27] C.G. Durfee *et al.*, Phys. Rev. Lett. **83**, 2187 (1999).
[28] E. Takahashi *et al.* (unpublished).
[29] Ph. Balcou *et al.*, in *Multiphoton Processes*, edited by Louis F. Di Mauro, Richard R. Freeman, and Kenneth Kulander, AIP Conf. Proc., No. 525 (AIP, Melville, NY, 2000), p. 319.
[30] M. Bellini *et al.*, Phys. Rev. A **64**, 023411 (2001).